# A Distributed Formation-Based Odor Source Localization Algorithm - Design, Implementation, and Wind Tunnel Evaluation

Jorge M. Soares, A. Pedro Aguiar, António M. Pascoal and Alcherio Martinoli

***Abstract*— Robotic odor source localization is a promising tool with numerous applications in safety, search and rescue, and environmental science. In this paper, we present an algorithm for odor source localization using multiple cooperating robots equipped with chemical sensors. Laplacian feedback is employed to maintain the robots in a formation, introducing spatial diversity that is used to better establish the position of the flock relative to the plume and its source. Robots primarily move upwind but use odor information to adjust their position and spacing so that they are centered on the plume and trace its structure. Real-world experiments were performed with an ethanol plume inside a wind tunnel, and used to both validate the algorithm and assess the impact of different formation shapes.**

## I. Introduction

In the aftermath of many armed conflicts, leftover mine fields represent a critical danger for local populations. Clearing these fields presents a model scenario for robotic chemical source tracking, bringing together a difficult detection environment and one that is dangerous to navigate, with risk of loss of life. Nonetheless, it is only one of many, among more common applications such as gas leak detection or search and rescue operations.

Over the past decade, we have witnessed significant evolution in the field of robotic olfaction, looking to address the above and other scenarios. Simple algorithms based on the behavior of insect species gave way to a host of approaches of differing complexity and inspiration, including not only a wide variety of bio-inspired algorithms but also those based on probabilistic inference, optimization meta-heuristics, or multi-robot swarms.

A common difficulty affecting all these solutions is the limited quantity and quality of information that can be collected by a single sensor. While this can be partially ascribed to what is still relatively early-stage sensing technology, it is also a consequence of the phenomenon under study. Odor propagation is, in effect, non-trivial, with concentration distribution being far from a smooth gradient [1]. Instead, odor arrives in packets, leading to wide fluctuations in the measured concentrations. Plumes are also dynamic and subject to meandering, i.e. their shape and position is continuously varying.

This paper expands on the work in odor plume tracing previously introduced in [2]. We present an improved distributed algorithm to lead a group of robots to the source of a chemical plume in stable wind conditions. By using multiple robots, we achieve spatial diversity in the odor sampling, providing us with more information than a single robot could collect. Having robots distributed along the crosswind direction makes it possible, over time, to estimate the relative position of the formation in the plume. Upwind diversity, less obvious in its advantages, still provides us with additional data points that may be averaged, becoming in a way analogous to temporal diversity and helping to overcome the patchiness of the plume.

Wind takes a central role in our solution. As odor tends to travel downwind, the direction of the wind provides a strong indication as to the relative position of the source. Accordingly, robots favor moving upwind when in the plume. Furthermore, we do not assume knowledge of either global position (e.g., GPS) or alignment (e.g., magnetic compass), and so the perceived direction of the wind becomes the only common reference for alignment. Relative position measurements enable a Laplacian feedback controller to maintain the robots in an arbitrary desired formation, and odor measurements are exchanged and used to drive the fleet to and along the center of the plume.

We perform real-world experiments in a wind tunnel, using Khepera III robots, building upon simulation experiments previously reported. The algorithm is fully distributed and self-contained, with no dependency on off-board information or processing. Wind direction, odor sensing, and inter-robot relative positioning leverage dedicated custom hardware designed at DISAL. In these experiments, we show that the algorithm can quickly converge to the desired formation and to the plume, and track it to its source.

The paper is organized as follows: in Section II we briefly review some of the related literature on this subject; in Section III we introduce the target hardware and environment for the experiments; in Section IV we present the details of our algorithm; in Section V we describe the wind tunnel experiments and the results obtained. Finally, in Section VI, we present our conclusions and ideas for future work.

## II. Related work

A survey of previous research in odor source localization and mapping can be found in [3], where a comprehensive taxonomy is defined and a multitude of solutions are discussed.

J. M. Soares and A. Martinoli are with the Distributed Intelligent Systems and Algorithms Laboratory, School of Architecture, Civil and Environmental Engineering, École Polytechnique Fédérale de Lausanne (EPFL), 1015 Lausanne, Switzerland.

J. M. Soares, A. P. Aguiar and A. M. Pascoal are with the Laboratory of Robotics and Systems in Engineering and Science, Instituto Superior Técnico, University of Lisbon, Av. Rovisco Pais, 1049-001 Lisboa, Portugal.

A. P. Aguiar is with the Research Center for Systems and Technology, Faculty of Engineering, University of Porto, Rua Dr. Roberto Frias, 4200-465 Porto, Portugal.

This work was partially funded by project FCT [UID/EEA/5009/2013] and grant SFRH/BD/51073/2010 from Fundação para a Ciência e Tecnologia.

Some of the simplest algorithms are inspired by the strategies used by biological agents such as bacteria [4] or silkworm moths [5], and usually consist of a set of basic states with associated behaviors. These include, for instance, moving upwind when inside the plume and moving in spirals when the plume is lost. Braitenberg-type approaches have also been tested successfully [6]. Experiments conducted with multiple robots [7], [8] have yielded mixed results, with authors reporting no clear improvement in the plume traversal phase, particularly in the absence of explicit collaboration [9].

Formation- and swarm-based algorithms [10], [11] are designed for cooperative multi-robot scenarios and work by coordinating the movement of several agents distributed over the area of interest. The information gained from simultaneous sampling at multiple locations and the close cooperation between the robots can greatly increase the efficiency of these approaches, while retaining computational simplicity. Our work was originally inspired by the crosswind formation algorithm presented in [12].

Of the more complex approaches, probabilistic inference methods have been been used extensively [9], [13]–[15]. Using multiple odor samples obtained over time and space and a model of plume propagation, agents are able to generate a probability distribution for the source location. This estimate is then used to compute movement steps or trajectories. Meta-heuristic optimization methods applied to the problem include Particle Swarm Optimization (PSO) [16]–[18], Ant Colony Optimization (ACO) [19], and others [20].

## III. Hardware and setup

### A. Robots

The algorithm was designed to target the limited capabilities of the Khepera III robots [21] used in the experiments. The Khepera III, produced by K-Team, is a small differential drive robot with a diameter of 12 cm. The robots are equipped with the Korebot II extension board, which features an Intel XScale PXA-270, 64 MB of Flash memory and 128 MB of RAM, and runs a GNU/Linux OS.

Sensor-wise, the base package includes a ring of infrared sensors, a pair of downward-facing infrared sensors, and a set of ultrasound proximity sensors. The wheels are equipped with high-resolution encoders and, for communication, an 802.11b CF card is installed.

### B. Additional sensing modules

The robots are equipped with a set of sensor boards allowing for an autonomous solution with no external dependencies. These sensors are installed in the form of three stacked add-on boards previously developed at DISAL, connected through the $I^2C$ bus available on the robots.

The wind direction sensing board [9] consists of a ring of six Honeywell 111-202CAK-H01 NTC thermistors in a star-shaped 3D-printed enclosure. The board uses an individually calibrated log-likelihood model to estimate the wind direction. Accuracy depends on the characteristics of each specific board and varies for particular angles, but the standard error for a well-built and well-calibrated board is approximately 5-8 deg, normally distributed, measured over the whole range. In reality, sensor error varies significantly across different boards and its distribution depends on the angle of incidence.

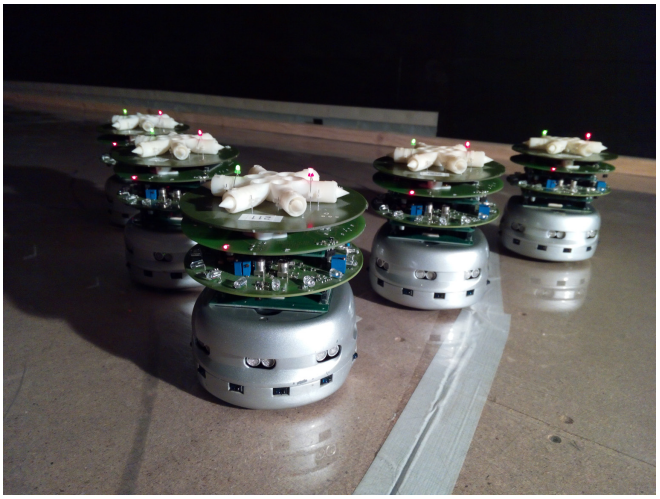

Fig. 1. Khepera III robot fleet. The robots are equipped with a wind sensing board (top), odor sensing board (middle) and relative localization board (bottom). The wind sensing board features red and green LEDs for overhead tracking.

The odor sensing board [9] features a MiCS-5521 volatile organic compound (VOC) resistive sensor from SGX Sensortech. A small pump continuously drives air through the sensor package, resulting in comparatively short (sub-second) response times. No response calibration was performed for the VOC sensors. Instead, before each experiment, sensors are left to measure and average their readings over a 3-minute period, leading to an approximate baseline that is then subtracted from the measurements taken during experiments.

Inter-robot relative positions are provided by an infrared range and bearing board [22]. The board employs a ring of 16 LED infrared emitters and 8 receivers to estimate the distance (from the received signal strength) and bearing (from the receivers the signal is reaching) to each neighbor. The transmitted signal encodes the sender ID so relative positions can be matched to a specific neighbor. The boards were configured to transmit at 10 Hz, and calibrated according to the procedure outlined in [23], with typical resulting standard errors of 10 % in range and 0.15 rad in bearing.

### C. Wind tunnel

The wind tunnel facility, shown in Fig. 2, is approximately 20 m long, 4 m wide, and 2 m high. Due to the construction of the tunnel and other equipment installed in the channel, the usable volume for our experiments is approximately 12 m x 3.5 m x 1.6 m. The reference frame $(x'-y')$ is placed at the upwind end of the wind tunnel. The $x'$ axis points downwind while the $y'$ axis points 90 ° counter-clockwise.

Tracking is accomplished by SwisTrack [24] and a six GigE camera setup designed to detect two color LEDs on the robots. The particles from the six cameras are merged in order to output a single position estimate for each robot. The low ceiling demands the use of wide-angle lenses that

Fig. 2. The wind tunnel used for the experiments. The odor outlet hose is at the opposite end, centered on the floor.

in turn introduce significant optical distortion. Nevertheless, local positioning error in most of the tunnel is around or below 8 cm, although significant jitter can be observed in areas of transition between cameras.

The experiments use a pure ethanol plume, generated by a low-speed pump circulating 1.2 l/min of room air through an A15 absolute alcohol reservoir, which evaporates spontaneously (at room temperature). We cannot control or measure the ethanol concentration at the outflow, but it can be assumed constant throughout an experiment. The 1 cm wide outlet is positioned at coordinates $(0.7\mathrm{m}, 1.9\mathrm{m})$, at floor level.

## IV. Technical approach

Our approach, first detailed in [2], is based on two key ideas. The first is that the wind direction provides an important hint as to the direction of the plume source. This is especially true for the near-laminar flow scenario in which we operate. The second is that multiple robots spread around the environment allow us to better determine the location of the odor plume and trace it to its source.

Our solution implements these two ideas in a three-component distributed controller running on each robot. The robots establish a formation, using a graph-based control framework and an arbitrary formation shape defined *a priori*, and move together towards the direction of the incoming wind. The odor readings obtained by each robot are used to center the entire formation in the observed plume and to scale the formation in order to better trace its structure. The algorithm runs at 10 Hz.

We briefly summarize the construction of the solution in the following section, but refer the reader to [2] for further details. Note, however, that the $x-y$ frame used in this work has been rotated in relation to the previous publication.

### A. Algorithm overview

The algorithm consists of three parallel behaviors, each generating a desired $(\dot{x},\dot{y})$ velocity vector. These components deal with upwind movement, formation control, and plume centering, and generate reference velocity vectors respectively denoted $\mathbf{u_w}$, $\mathbf{u_f}$ and $\mathbf{u_c}$. These vectors are then combined and transformed to regulate the movement of the robot.

Wind plays a crucial role in our solution. Due to the error inherent to wind sensing, the measurements coming from the wind sensor board and the odometry information from the wheel encoders are fused by a Kalman filter, yielding $\theta$, an estimate of the true wind direction. At the most basic level, the algorithm uses this information to bias the motion towards the perceived upwind direction:

$$\mathbf{u_w} = R(\theta)\begin{bmatrix}1\\0\end{bmatrix} \tag{1}$$

As we intend for the formation to be aligned with the wind, the same rotation $R(\theta)$ is also used throughout the algorithm, in formation keeping and plume centering, as a coordinate transformation from the $upwind-crosswind$ wind frame to the $x-y$ robot frame. In effect, the wind serves as our sole source of global alignment information.

The formation can be formalized as an undirected graph $G=(V,E)$, in which vertices $V$ correspond to robots and edges $E$ correspond to inter-robot relative positioning links. Convergence to a desired formation can, for a fully connected graph of holonomic robots modeled as single integrators, be achieved locally with the following controller:

$$\mathbf{u_f} = -\begin{bmatrix}\sum_{j=0}^{N}\mathcal{L}_j\left(x_j-\beta_j^x\right)\\ \sum_{j=0}^{N}\mathcal{L}_j\left(y_j-\beta_j^y\right)\end{bmatrix} \tag{2}$$

where $x_j$ and $y_j$ are the relative positions to robot $j$ in the body frame and $\mathcal{L}_j = \mathcal{L}_{i,j}$ is the entry of the positive-semidefinite Laplacian matrix, $\mathcal{L}=\mathcal{B}\mathcal{B}^T$, that relates controlled node $i$ to neighbor $j$.

The formation shape is specified by two bias vectors, describing the position of each robot in the formation, in the wind frame. $\beta_j$ describes the desired spacing between robots $i$ and $j$ in the robot frame, i.e. $\beta_j = R(\theta_i)S[\bar{\mathbf{p}}_\mathbf{j}-\bar{\mathbf{p}}_\mathbf{i}]$, $\bar{\mathbf{p}}_\mathbf{j}$ and $\bar{\mathbf{p}}_\mathbf{i}$ the absolute offsets in the wind frame.

The adaptive bias matrix $S=\mathrm{diag}(s_{uw},s_{cw})$ groups two scalar parameters that represent scaling factors in the upwind and crosswind directions. As the structure of the plume does not change significantly in the upwind direction, we use a constant upwind scaling factor and vary the crosswind scale using a proportional controller on the difference between the center concentration ($c_c$) and the sum of the left- and right-side concentrations ($c_l$ and $c_r$, respectively):

$$\dot{s}_{cw} = k_{cw}((c_l+c_r)-c_c) \tag{3}$$

The underlying goal is to keep the formation span such that the side robots are each detecting approximately half of the center concentration, thereby tracing the shape of the plume. The range of $s_{cw}$ is limited in order to maintain the robots at a safe distance and within the dimensions of the tunnel. The proportional gain $k_{cw}$ need not be precisely tuned, provided its magnitude yields small enough step variations.

We also require the formation to remain centered in the plume. To that end, we use a crosswind alignment component dependent on the difference between the average concentrations detected by robots on the left and right sides of the formation. To prevent rapid variations in control outputs due to the high amplitude of odor measurements, we implement a generalized logistic response given by

$$\mathbf{u_c} = R(\theta)\begin{bmatrix} 0 \\ -u_c^{max} + \frac{2u_c^{max}}{1+e^{-(c_l-c_r)/k_l}} \end{bmatrix} \tag{4}$$

In all experiments, $u_c^{max}$ is set to $0.25$, the maximum crosswind speed that may be requested by the centering behavior. The constant $k_l$ depends on the dynamic range of the sensor and affects the smoothness of the response. The velocity vectors for each component are combined using a weighted sum:

$$\mathbf{u} = k_w\mathbf{u_w} + k_c\mathbf{u_c} + k_f\mathbf{u_f} \tag{5}$$

In our experiments, we use constant weights $k_w = k_c = k_f = 1$, but these can be tuned, possibly dynamically, to vary the importance of each behavior, e.g. to prioritize maintaining a rigid formation even at the expense of quick reaction to changes in the plume.

As we work with nonholonomic differential drive robots, the vector $\mathbf{u} = \begin{bmatrix} u_x & u_y \end{bmatrix}^T$ is translated into requested linear and angular speeds using simple proportional controllers limited to forward movement and saturated to a target top speed, that is,

$$v = k_v u_x \qquad 0 \le v \le v_{max} \tag{6}$$

$$\omega = k_\omega u_y \qquad -\omega_{max} \le \omega \le \omega_{max} \tag{7}$$

### *B. Improvements over simulation version*

While the core ideas of the algorithm have not suffered any changes, improvements were made in order to better cope with real-world conditions. These included an assortment of simple changes: a new proportional controller for the scaling factor, an improved Kalman filter for wind direction that takes advantage of the existing Khepera III odometry tracking framework, and an improved max filter for the odor measurements that also reduces window size, taking into account the on-board integration and sensor recovery time.

The most significant changes took place in the handling of relative positions. In our simulation work, relative positions were available at every time step and to every other robot, which is not the case in reality. Occlusion is a problem, and manifests itself in either the absence of measurements or the measurement of consistently larger distances due to attenuation or reflection. Trivial solutions consist of considering all recent measurements (susceptible to indirect detections) and only considering measurements to robots for which edges exist in a static graph (standard graph-based formation control).

We hybridize these strategies and consider both edges in the graph and robots that are close enough to manifest a collision risk and thus unlikely to be indirect detections. This yields two advantages: protection against spurious measurements that may destabilize the formation, and collision avoidance to every robot, regardless of it being a neighbor in the graph. The implementation was also changed to only consider recent measurements, i.e. those obtained within the last 3 cycles.

Due to component tolerances, no two relative position boards transmit at the exact same power level. This translates into a situation in which two boards at the same physical distance will be detected at different ranges. As two neighboring robots will not perceive the same distance to each other, this creates a situation in which one will tend to chase the other. To cope with it, each robot broadcasts its measured range to its neighbors. The robot's own measurements and those received from its neighbors are averaged and used for formation control. This guarantees that two neighboring robots see one another at the same distance.

## V. WIND TUNNEL EXPERIMENTS

A set of experiments were run using the hardware and infrastructure described in Section III. In all experiments, the wind speed is set to approximately 1 m/s. At the start of a series, the odor baseline for each robot is obtained, after which the odor source is activated. Robots are placed at the opposite end of the tunnel, approximately 13 m downwind from the source and in different initial configurations, and the algorithm is started.

Plume finding being outside the scope of this work, robots are expected to start in the vicinity of the plume. The only requirement is, however, that a single robot remains in the plume, whereas the others may be outside its influence. Source declaration is also not addressed; experiments are manually stopped once the robots approach the source's end of the channel.

Individual experiments last approximately three minutes: although the exact time to completion depends on all three behaviors, it is primarily influenced by the intensity of the upwind bias and the parameters of the speed controller, both kept constant throughout the evaluation. In the course of the experiments, we witnessed no failures to find the source attributable to the algorithm; all observed cases were due to hardware faults.

For the first series of experiments, five nodes were configured with the formation shown in Fig. 3. Each node is an endpoint to three edges in the graph, corresponding to the three relative positions the robot will generally consider for formation control purposes.

Figure 4 shows the results of three separate runs. The robots start on the right side of the plot, in three different starting configurations: a crosswind line to the right of the plume center (top), a crosswind line to the left of the plume center (middle) and arbitrarily distributed in the environment (bottom). They converge to the desired formation as they move towards the source, represented by the black square on the left side. A video portraying these experiments is provided in the accompanying material to this paper.

The trajectories show the robots quickly approaching the desired formation, and reducing the crosswind spacing (i.e., narrowing the formation shape) as they approach the source.

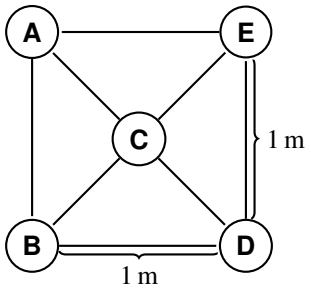


Fig. 3. Five-node square formation showing graph edges and base distances. Actual desired distances are dynamically varied by the algorithm.

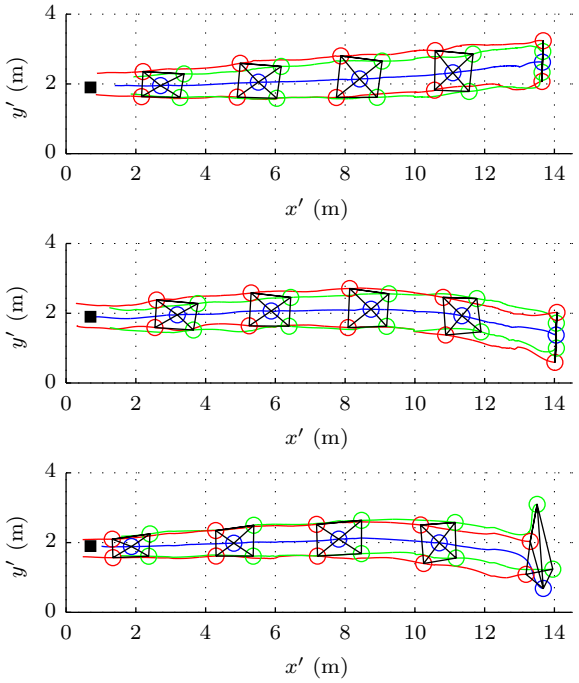


Fig. 4. Trajectories obtained using the 5-robot square formation, for three different sets of starting positions. Black lines are plotted connecting the robot positions every 40 seconds, and the odor source is represented by the black square (size not to scale) on the left side.

The remaining formation error is mostly due to the aforementioned systematic error in relative positioning and, to a certain extent, inaccurate wind measurements. Some observed jitter corresponds to noise introduced by the tracking system.

Additional experiments were run for three different formations: a five-robot inverted V formation (Fig. 5a), a three-robot linear formation (Fig. 5b), and a three-robot inverted V formation (Fig. 5c). Three experiments were run in each case, with robot starting positions following the same recipe as for the first formation.

The outcomes do not differ substantially as a result of the starting conditions, therefore a single example run for each formation is shown in Fig. 6. Table I summarizes the quantitative results obtained in the experiments. The movement overhead is defined as $\alpha = d/\Delta - 1$, where $d$ is the actual distance traveled by the formation centroid (i.e., the Riemann sum of its discrete step position variations)

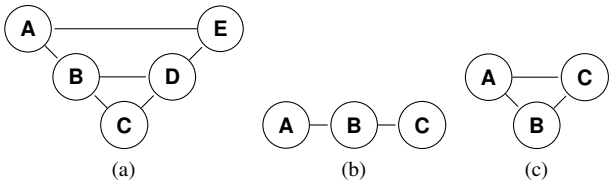


Fig. 5. Alternative formations: (a) five-robot inverted V formation; (b) three-robot linear formation; (c) three-robot inverted V formation

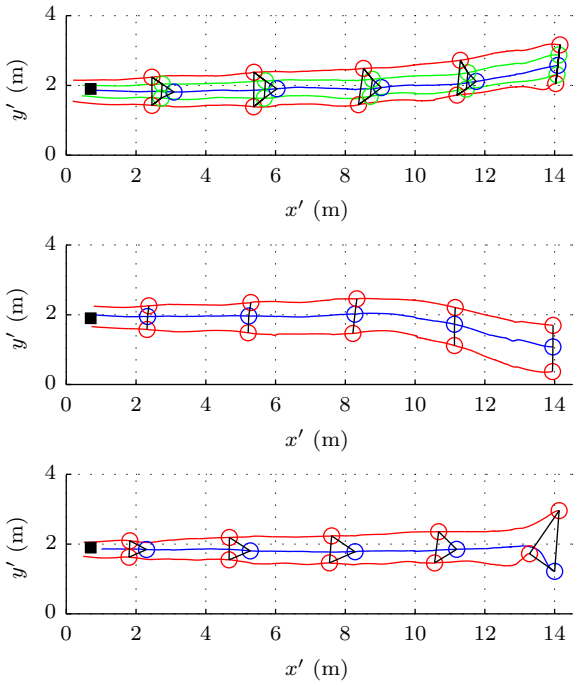


Fig. 6. Example trajectories obtained using the alternative formations, in the same order. Black lines are plotted connecting the robot positions every 40 seconds, and the odor source is represented by the black square (size not to scale) on the left side.

TABLE I

MOVEMENT OVERHEAD AND FINAL ERROR OBTAINED FOR EACH EXPERIMENT.

| | | 5 robots | | 3 robots | |
|---|---|---|---|---|---|
| | | Square | Inv. V | Linear | Inv. V |
| E1 | $\alpha$ | 0.30% | 0.32% | 0.42% | 0.89% |
| | $\epsilon$ | 0.05 m | 0.04 m | 0.04 m | 0.01 m |
| E2 | $\alpha$ | 0.78% | 0.97% | 1.01% | 0.35% |
| | $\epsilon$ | 0.04 m | 0.06 m | 0.10 m | 0.04 m |
| E3 | $\alpha$ | 0.38% | 0.34% | 0.51% | 0.24% |
| | $\epsilon$ | 0.01 m | 0.04 m | 0.01 m | 0.04 m |

and $\Delta$ is the norm of its displacement (i.e., the straight-line distance between starting and final positions). The error is given by $\epsilon = |x_c - x_s|$, the distance between the crosswind positions of the center robot at the final coordinate ($x_c$) and that of the source ($x_s$). Prior to metric calculation, tracks are fed to a low-pass filter to remove SwisTrack noise; this operation does not substantially distort the actual trajectories, as system dynamics occur at lower frequency.

While the number of runs does not allow us to draw statistically significant conclusions for each scenario, the

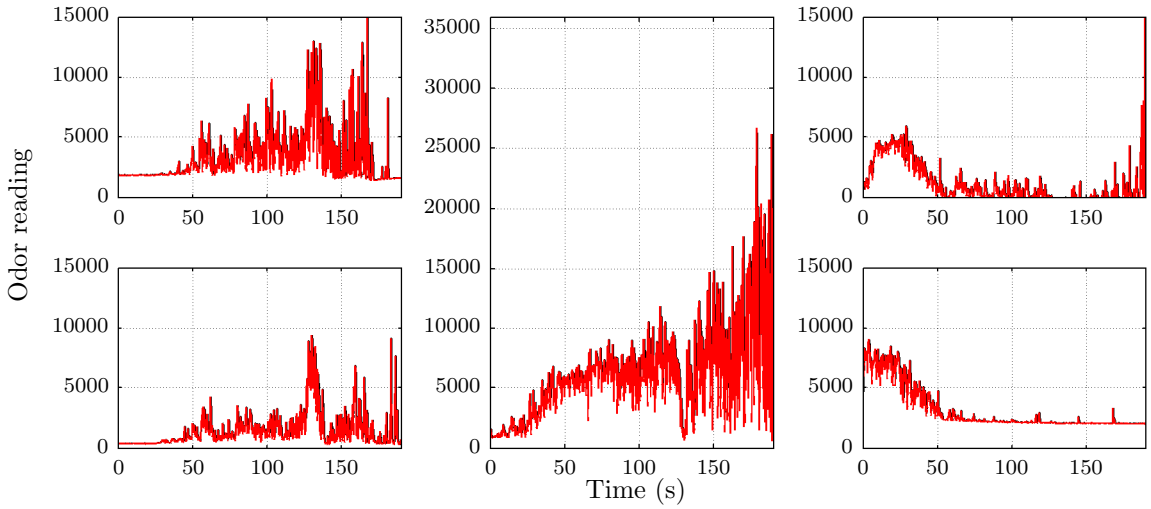


Fig. 7. Odor measurements (arbitrary units) obtained along the path during a complete experiment with 5 robots in a square formation, starting on the left side of the plume. The plot position matches the robot positions, i.e. the top left plot corresponds to the forward left robot.

average performance of the algorithm across the whole sample is $\bar{\alpha}=0.54\%$,$\sigma_\alpha=0.28$ and $\bar{\epsilon}=0.04\text{m}$,$\sigma_\epsilon=0.03$. The results suggest that, in the vast majority of cases, the robots will trace the plume to a neighborhood of the source smaller than one robot diameter, and do so while covering only a slightly longer distance than the optimal straight-line path.

Figure 7 shows the odor measurements obtained by each robot during the second experiment with the 5-robot square formation. The plot positions correspond to the formation positions as defined in Fig. 3. As the robots start on the left side of the plume, an initial period of higher readings for right-side robots (and, conversely, an initial period of very low readings for left-side robots) can be observed. It is important to note that, despite the trend for increasing readings, particularly in the case of the center robot, the signal shows extreme variations.

Figure 8 shows the wind direction estimates for each robot, generated by the Kalman filter based on wind measurements and odometry information. Even post-filtering, both low- and high-frequency noise are non-negligible. Furthermore, one of the sensors is biased, returning consistently elevated measurements. Nevertheless, by explicitly and implicitly capitalizing on information from all the robots, the algorithm is able to better cope with imperfect sensing. While no data for the relative positioning board is shown, the combination of the high connectivity of the formation graph and the range exchange and averaging mechanism is also robust against measurement inaccuracies.

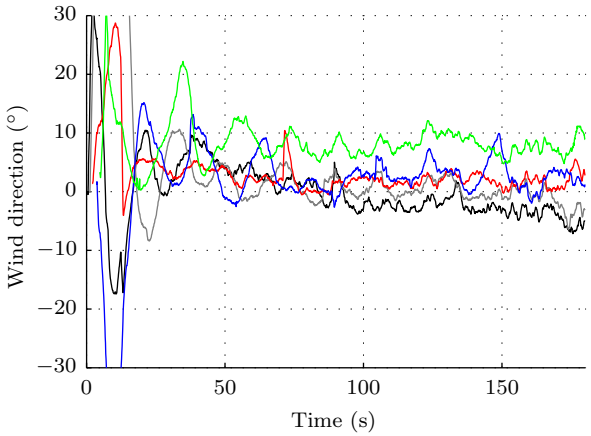


Fig. 8. Filtered wind direction estimates obtained for each robot during a complete experiment with 5 robots in a square formation.

## VI. Conclusions and Outlook

This paper discussed an approach for odor source localization using multiple cooperative robots. In this solution, robots move upwind in an arbitrary formation, collecting and sharing odor data that are used to optimize the formation shape, center the robots on the plume, and follow the plume to its source. The solution is distributed and fully self-contained, exploiting only the sensors deployed on the robots and requiring no external hardware or support. We introduced changes to the algorithm that, however small, are key to coping with realistic conditions that were not modeled in simulation, allowing us to handle even more intermittent odor distributions, unreliable sensing, and systematic errors.

The resulting solution was subject to validation and evaluation with real robots. Multiple experiments were run using an ethanol plume in a wind tunnel environment, allowing us to measure and study the behavior and performance of the algorithm. Results show that we are able to reach the source with minimal distance overhead ($\bar{\alpha} = 0.54\,\%$), performing better than comparably simple single-robot bio-inspired algorithms [9]. While there are increased financial and energy costs associated with employing multiple robots, the high efficiency is a clear advantage for critical missions where time is of the essence.

In the future, we plan to further explore the performance impact of different formation shapes in systematic simulation and experimentation, taking advantage of the flexibility of the algorithm. We also plan to extend the solution to robots capable of 3D movement, and investigate mechanisms for robustness to failure of individual robots through adaptive formation reshaping.

One clear limitation of our algorithm is its reliance on knowledge of the wind direction. This makes it inapplicable to low wind scenarios, where chemical transport is diffusion-dominated and, furthermore, accurately estimating the wind direction may prove difficult. It also raises questions about its performance in highly turbulent flows, where an unsteady wind signal and more complex chemical field will, in principle, increase the time taken to find the source and lead to higher failure rates. In spite of the additional complexity, the use of multiple distributed sensing agents may still present an advantage when compared to other solutions. We intend to explore this question and devise alternative formulations better suited to tackling these scenarios.

## REFERENCES


[1] P. J. W. Roberts and D. R. Webster, *Turbulent diffusion*. ASCE Press, Reston, Virginia, 2002.

[2] J. M. Soares, A. P. Aguiar, M. Pascoal, and A. Martinoli, "A graph-based formation algorithm for odor plume tracing," in *International Symposium on Distributed Autonomous Robotic Systems*, Daejeon, South Korea, Nov. 2014, p. [To appear].

[3] G. Kowadlo and R. Russell, "Robot odor localization: a taxonomy and survey," *The International Journal of Robotics Research*, vol. 27, no. 8, pp. 869–894, Aug. 2008.

[4] A. Dhariwal, G. Sukhatme, and A. Requicha, "Bacterium-inspired robots for environmental monitoring," in *IEEE International Conference on Robotics and Automation*, 2004, pp. 1436–1443.

[5] L. Marques, U. Nunes, and A. T. de Almeida, "Olfaction-based mobile robot navigation," *Thin Solid Films*, vol. 418, no. 1, pp. 51–58, Oct. 2002.

[6] A. Lilienthal and T. Duckett, "Experimental analysis of gas-sensitive Braitenberg vehicles," *Advanced Robotics*, vol. 18, no. 8, pp. 817–834, Dec. 2004.

[7] A. Hayes, A. Martinoli, and R. Goodman, "Distributed odor source localization," *IEEE Sensors Journal*, vol. 2, no. 3, pp. 260–271, June 2002.

[8] A. Khalili, A. Rastegarnia, M. K. Islam, and Z. Yang, "A bio-inspired cooperative algorithm for distributed source localization with mobile nodes." in *Annual International Conference of the IEEE Engineering in Medicine and Biology Society*, Osaka, Japan, Jan. 2013, pp. 3515–8.

[9] T. Lochmatter, "Bio-inspired and probabilistic algorithms for distributed odor source localization using mobile robots," {PhD} Thesis 4628, École Polytechnique Federale de Lausanne, 2010.

[10] V. Genovese, P. Dario, R. Magni, and L. Odetti, "Self organizing behavior and swarm intelligence in a pack of mobile miniature robots in search of pollutants," in *IEEE/RSJ International Conference on Intelligent Robots and Systems*, vol. 3, 1992, pp. 1575–1582.

[11] A. Marjovi and L. Marques, "Optimal swarm formation for odor plume finding," *IEEE Transactions on Cybernetics*, vol. 99, no. 12, pp. 2302–2315, 2014.

[12] T. Lochmatter, E. Göl, I. Navarro, and A. Martinoli, "A plume tracking algorithm based on crosswind formations," in *International Symposium on Distributed Autonomous Robotic Systems*. Lausanne, Switzerland: Springer Tracts in Advanced Robotics (2013), Vol. 83, pp. 91-102, 2010.

[13] M. Vergassola, E. Villermaux, and B. I. Shraiman, "'Infotaxis' as a strategy for searching without gradients." *Nature*, vol. 445, no. 7126, pp. 406–9, Jan. 2007.

[14] J.-G. Li, Q.-H. Meng, Y. Wang, and M. Zeng, "Odor source localization using a mobile robot in outdoor airflow environments with a particle filter algorithm," *Autonomous Robots*, vol. 30, no. 3, pp. 281–292, Jan. 2011.

[15] J.-G. Li, J. Yang, J. Liu, G.-D. Lu, and L. Yang, "Odor-source searching using a mobile robot in time-variant airflow environments with obstacles," in *Chinese Control Conference*, Nanjing, China, July 2014, pp. 8559–8564.

[16] G. Cabrita, L. Marques, and V. Gazi, "Virtual cancelation plume for multiple odor source localization," in *IEEE/RSJ International Conference on Intelligent Robots and Systems*, Nov. 2013, pp. 5552–5558.

[17] W. Jatmiko, K. Sekiyama, and T. Fukuda, "A PSO-based mobile robot for odor source localization in dynamic advection-diffusion with obstacles environment: theory, simulation and measurement," *IEEE Computational Intelligence Magazine*, vol. 2, no. 2, pp. 37–51, 2007.

[18] L. Marques, U. Nunes, and A. T. Almeida, "Particle swarm-based olfactory guided search," *Autonomous Robots*, vol. 20, no. 3, pp. 277–287, May 2006.

[19] M.-L. Cao, Q.-H. Meng, X.-W. Wang, B. Luo, M. Zeng, and W. Li, "Localization of multiple odor sources via selective olfaction and adapted ant colony optimization algorithm," in *IEEE International Conference on Robotics and Biomimetics*, Dec. 2013, pp. 1222–1227.

[20] G. de Croon, L. O'Connor, C. Nicol, and D. Izzo, "Evolutionary robotics approach to odor source localization," *Neurocomputing*, vol. 121, pp. 481–497, Dec. 2013.

[21] A. Prorok, A. Arfire, A. Bahr, J. R. Farserotu, and A. Martinoli, "Indoor navigation research with the Khepera III mobile robot: an experimental baseline with a case-study on ultra-wideband positioning," in *International Conference on Indoor Positioning and Indoor Navigation*, Zurich, Switzerland, 2010, doi:10.1109/IPIN.2010.5647880.

[22] J. Pugh, X. Raemy, C. Favre, R. Falconi, and A. Martinoli, "A fast on-board relative positioning module for multirobot systems," *IEEE/ASME Transactions on Mechatronics*, vol. 14, no. 2, pp. 151–162, 2009.

[23] S. Gowal, A. Prorok, and A. Martinoli, "Two-phase online calibration for infrared-based inter-robot positioning modules," in *IEEE International Conference on Intelligent Robots and Systems*, 2011, pp. 3313–3319.

[24] T. Lochmatter, P. Roduit, C. Cianci, N. Correll, J. Jacot, and A. Martinoli, "SwisTrack - a flexible open source tracking software for multi-agent systems," in *IEEE/RSJ International Conference on Intelligent Robots and Systems*, 2008, pp. 4004–4010.